Electronic Supplementary Material (ESI) for Integrative Biology.

SUPPLEMENTAL INFORMATION

Microengineered cultures containing human hepatic stellate cells and hepatocytes for drug development

Matthew D. Davidson, David A. Kukla, and Salman R. Khetani

LIST OF ABBREVIATIONS

- **Alpha (α)-SMA**: alpha smooth muscle actin
- **CRP:** C-reactive protein
- **CYP3A4:** Cytochrome P450 3A4
- **DMSO:** dimethylsulfoxide
- **FXR:** farnesoid X receptor
- **GA HSCs:** Growth-arrested hepatic stellate cells
- **GAPDH:** Glyceraldehyde 3-phosphate dehydrogenase
- **GKT**: GKT137831
- **HPRT:** hypoxanthine-guanine phosphoribosyltransferase
- **HSCs:** Hepatic stellate cells (primary human)
- **IL-6:** interleukin-6
- **MPCCs:** Micropatterned co-cultures containing primary human hepatocytes patterned on collagen-coated domains and surrounded by growth-arrested 3T3-J2 fibroblasts
- **MPCC-HSC:** Micropatterned co-cultures containing primary human hepatocytes patterned on collagen-coated domains and surrounded by proliferating hepatic stellate cells.
- **MPCC-GA HSC:** Micropatterned co-cultures containing primary human hepatocytes patterned on collagen-coated domains and surrounded by growth-arrested (mitomycin C treatment) hepatic stellate cells.
- **MPTCs:** Micropatterned tri-cultures containing primary human hepatocytes patterned on collagen-coated domains and surrounded by a mixture of growth-arrested 3T3-J2 fibroblasts and primary human hepatic stellate cells
- **NFE2L2:** Nuclear factor Erythroid 2 like 2 (also known as Nrf2)
- **NOX1:** NADPH-oxidase 1
- **NOX4:** NADPH-oxidase 4
- **OCA:** obeticholic acid
- **PHHs:** Primary human hepatocytes

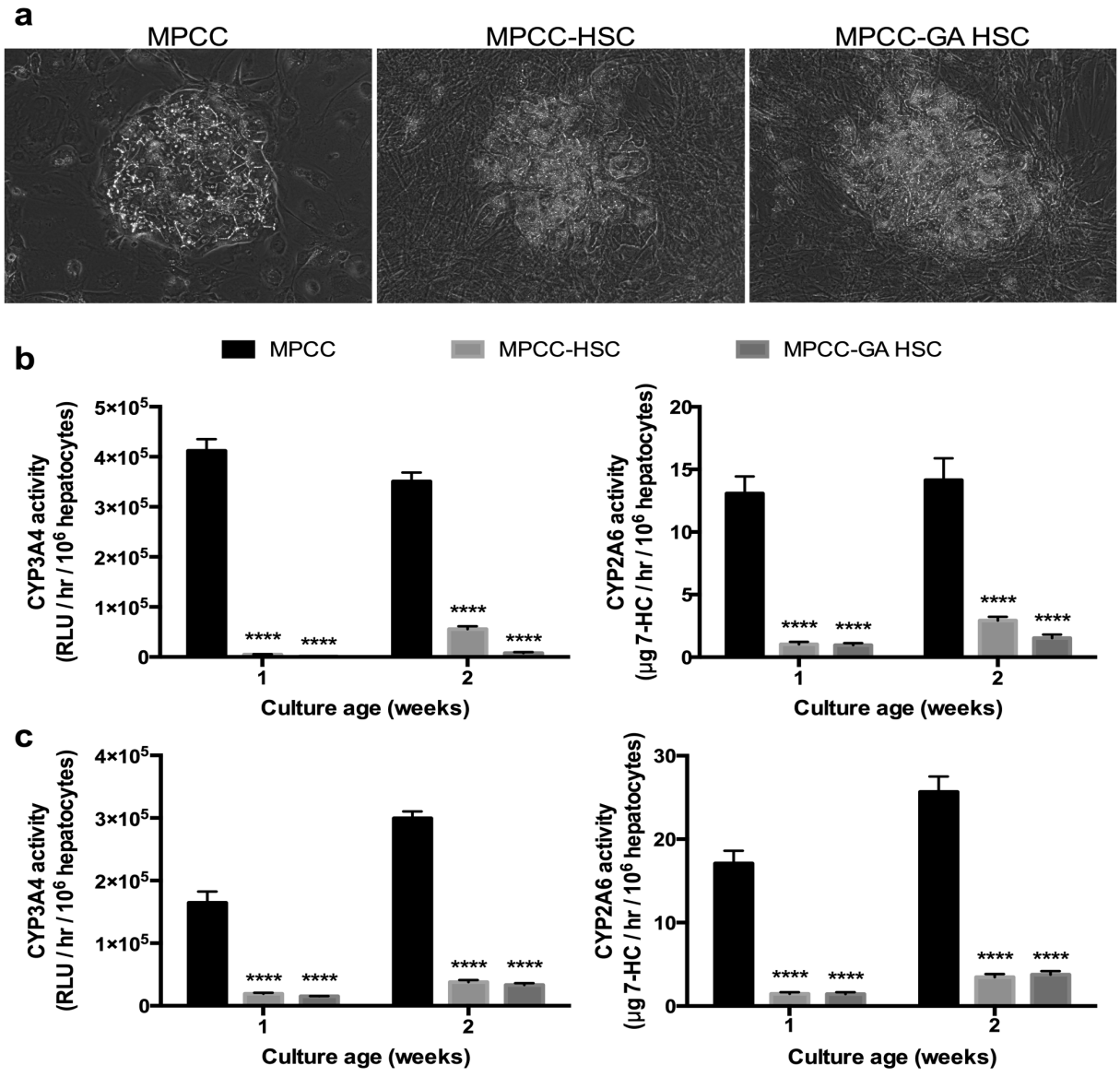

Supplemental Figure 1. Morphology and functions of PHHs cultured in MPCCs, MPCC-HSC or MPCC-GA HSC. (a) Phase contrast images of the different models at day 16. **(b)** CYP3A4 (left) and CYP2A6 (right) activities over time. **(c)** Similar data as in panel 'b' except a different PHH donor and different HSC donor were used to create the culture models. Statistical significance is displayed relative to MPCCs at a similar time-point. **** p≤0.0001.

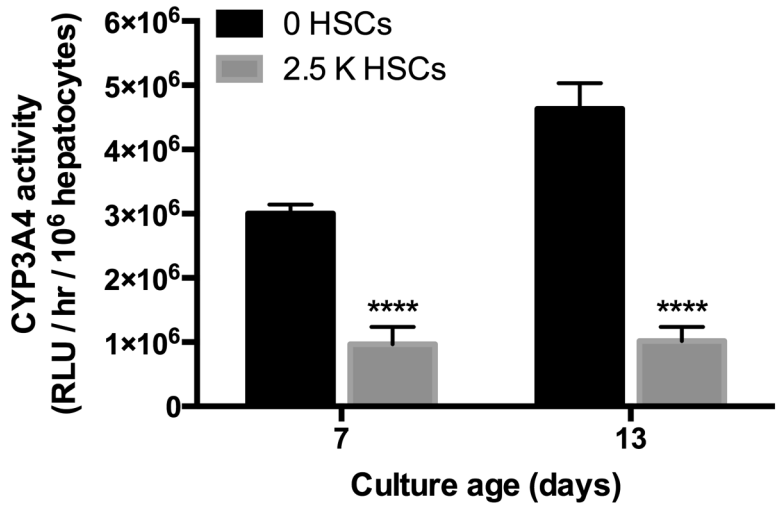

Supplemental Figure 2. Activated HSCs cause downregulation of CYP3A4 activity in PHHs within MPTCs. The 2.5K HSCs (proliferative) with 30K PHHs in a 24-well format corresponds to the approximate ratio in the human liver of 1 HSC to 12 PHHs (i.e. 5% HSCs and 60% PHHs of the total number of cells in the liver). Statistical significance is displayed relative to MPCCs at a similar time-point. **** p≤0.0001.

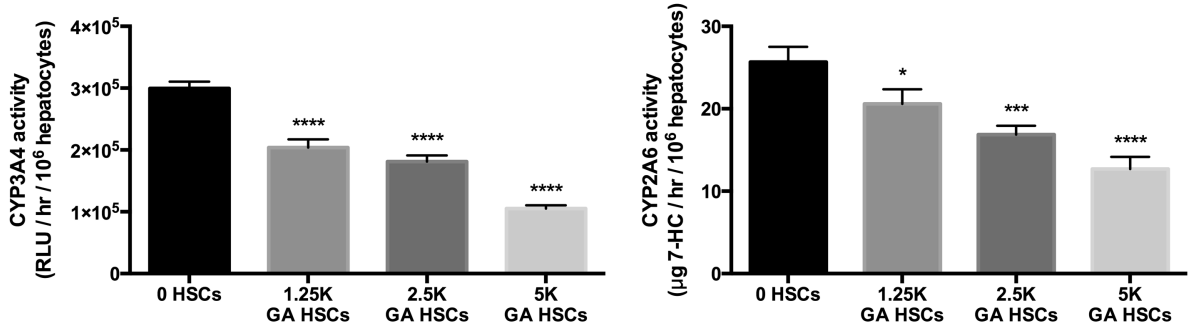

Supplemental Figure 3. Activated and growth-arrested HSCs cause downregulation of CYP3A4 and CYP2A6 activities in PHHs within MPTCs. HSCs were growth-arrested via mitomycin C treatment prior to incorporation into MPTCs. Data from day 16 of culture is shown. Statistical significance is displayed relative to MPCCs (0 HSCs). * p≤ 0.05, *** p≤0.001, and **** p≤0.0001.

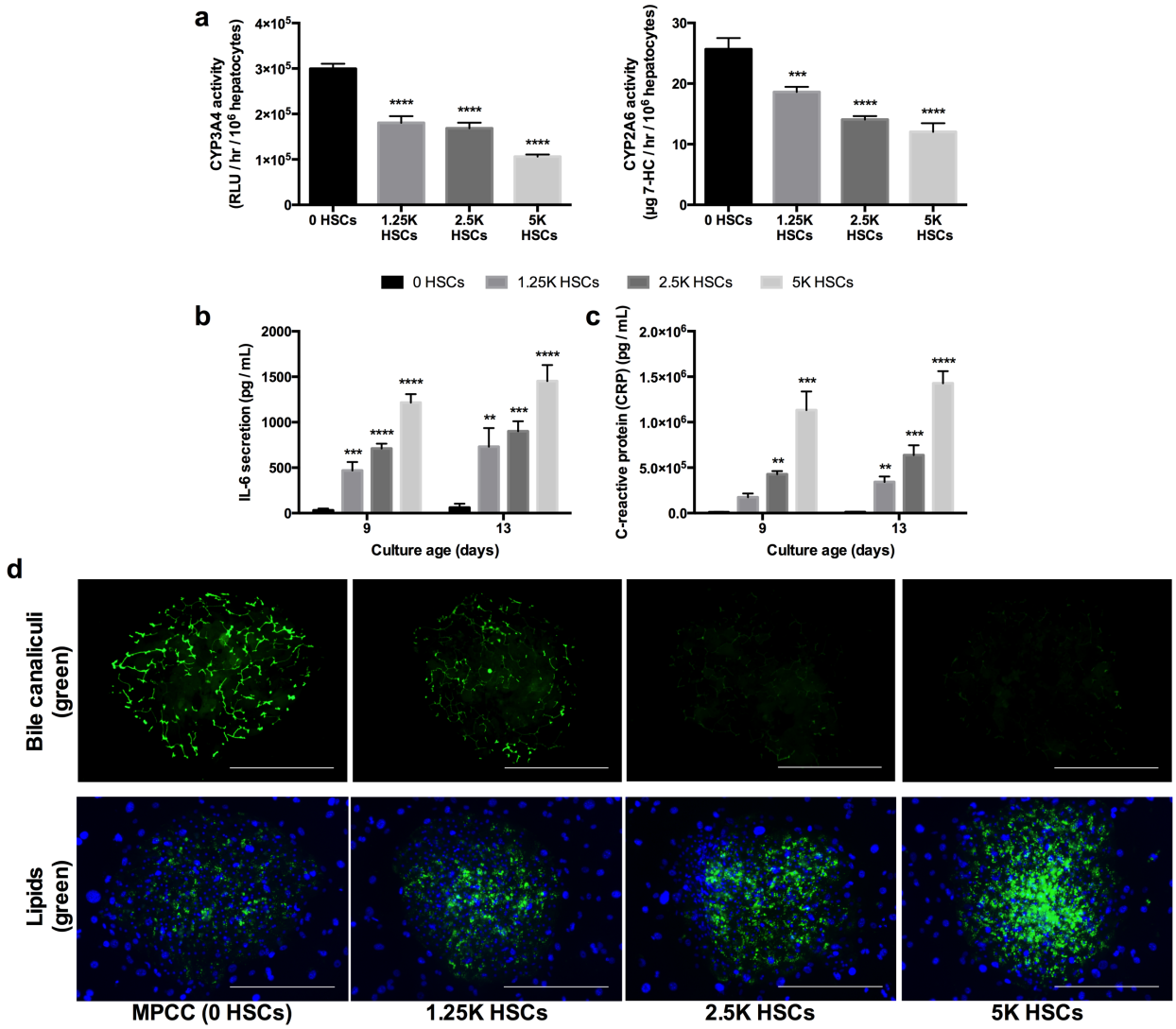

Supplemental Figure 4. Activated HSCs cause hepatic dysfunctions and increased production of IL-6 and CRP in MPTCs (cultures were created using different PHH and HSC donors than those featured in the main figures). **(a)** CYP3A4/2A6 activities in 7-day-old MPTCs and MPCCs (0 HSC). IL-6 (**b**) and CRP (**c**) levels in MPTCs and MPCCs. **(d) Top row:** Images of PHH islands in 15-day-old cultures showing export of (or lack thereof) fluorescent dye into the hepatic bile canaliculi. **Bottom row:** Nile red-stained PHH islands in 15-day-old cultures. Scale bars represent 400 µm. Statistical significance is displayed relative to MPCCs (0 HSCs) at the respective time-point. ** p≤ 0.01, *** p≤0.001, and **** p≤0.0001. Note: Quantification of HSC numbers within MPTCs from these donors is featured in main Figure 3D.

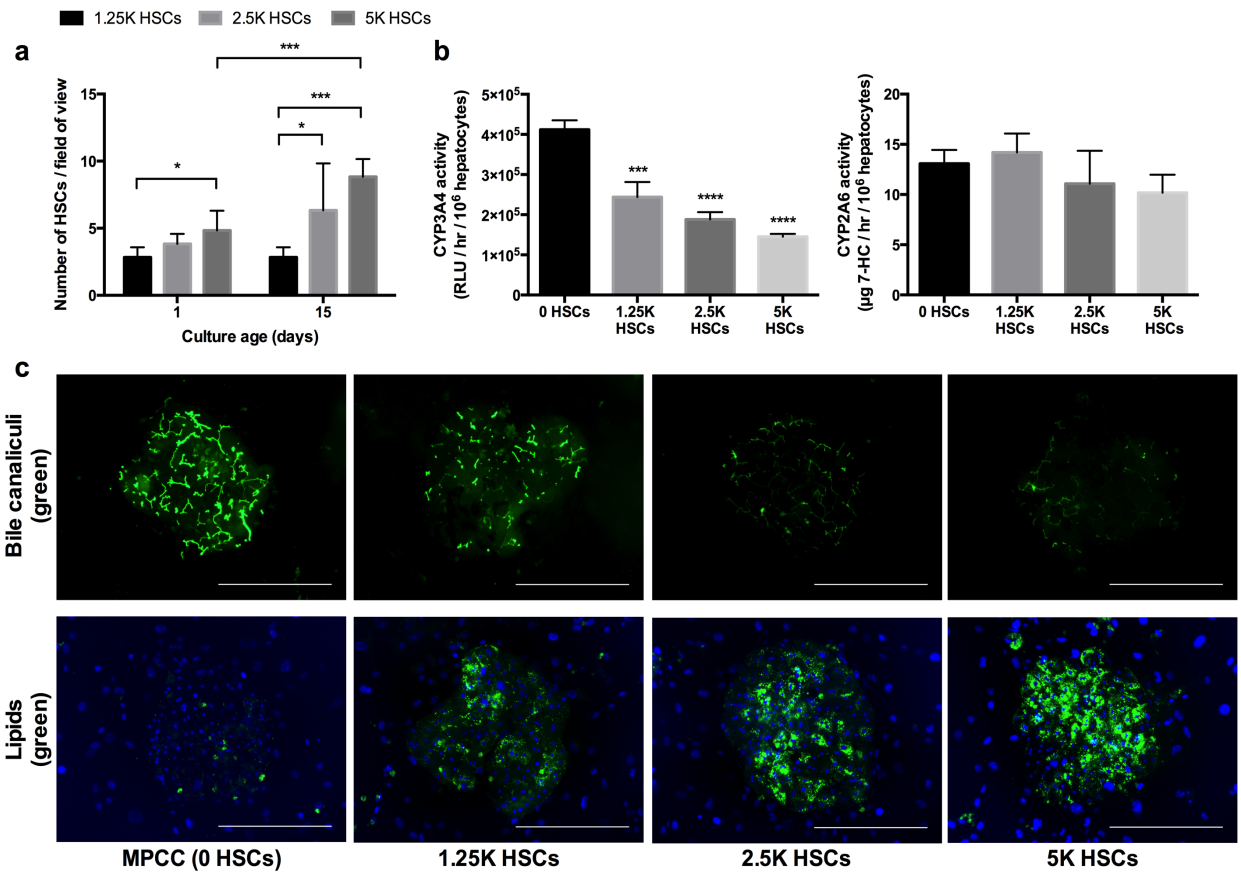

Supplemental Figure 5. Activated HSCs cause hepatic dysfunctions and increased production of IL-6 and CRP in MPTCs (cultures were created using different PHH and HSC donors than those featured in the main figures and those featured in supplemental figure 4 above). **(a)** An increase in α-SMA-positive HSC numbers within MPTCs over time. **(b)** CYP3A4/2A6 activities in 8-day-old MPTCs and MPCCs (0 HSC). **(c) Top row:** Images of PHH islands in 16-day-old cultures showing export of (or lack thereof) fluorescent dye into the hepatic bile canaliculi. **Bottom row:** Nile red-stained PHH islands in 16-day-old cultures. Statistical significance in panel 'b' is displayed relative to MPCCs (0 HSCs) at the respective time-point. * p≤ 0.05, *** p≤0.001, and **** p≤0.0001. Scale bars on images represent 400 µm. Note: IL-6 and CRP levels over time in supernatants from MPTCs and MPCCs from these donors is featured in main Figure 7.

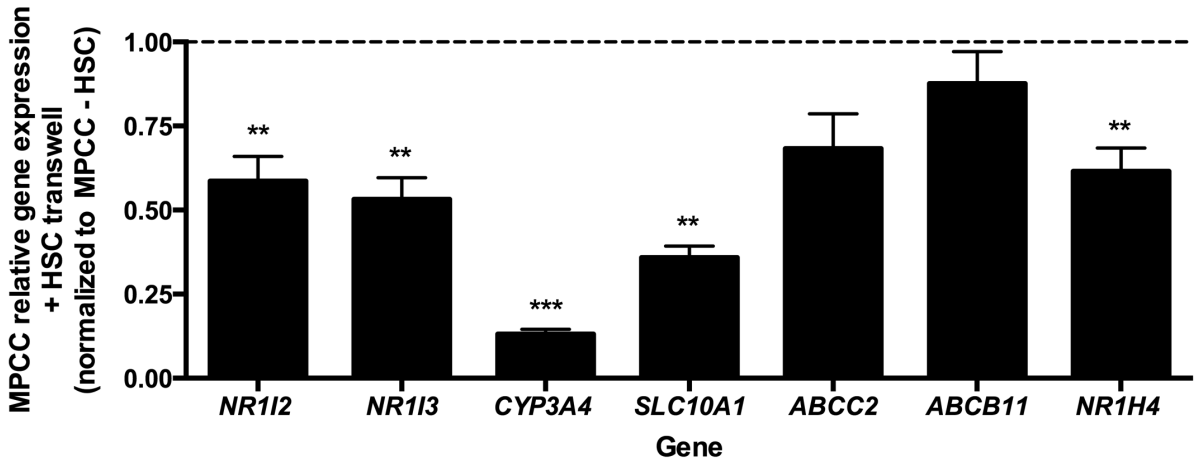

Supplemental Figure 6. Paracrine signaling with activated HSCs in a transwell configuration leads to downregulation of gene expression in PHHs within MPCCs (cultures were created using a different HSC donor than the one featured in the main figure 6). Transwell tri-cultures were created containing MPCCs on the bottom of the well and activated HSCs cultured in the insert placed on top within 1-2 days following the separate establishment of both MPCCs and HSC cultures. Gene expression after 2 weeks of culture in MPCCs cultured with HSC-containing inserts. Data is normalized to gene expression in MPCCs cultured with cell-free inserts. Statistical significance is displayed relative to MPCCs with cell-free transwell inserts. ** $p \leq 0.01$ and *** $p \leq 0.001$.

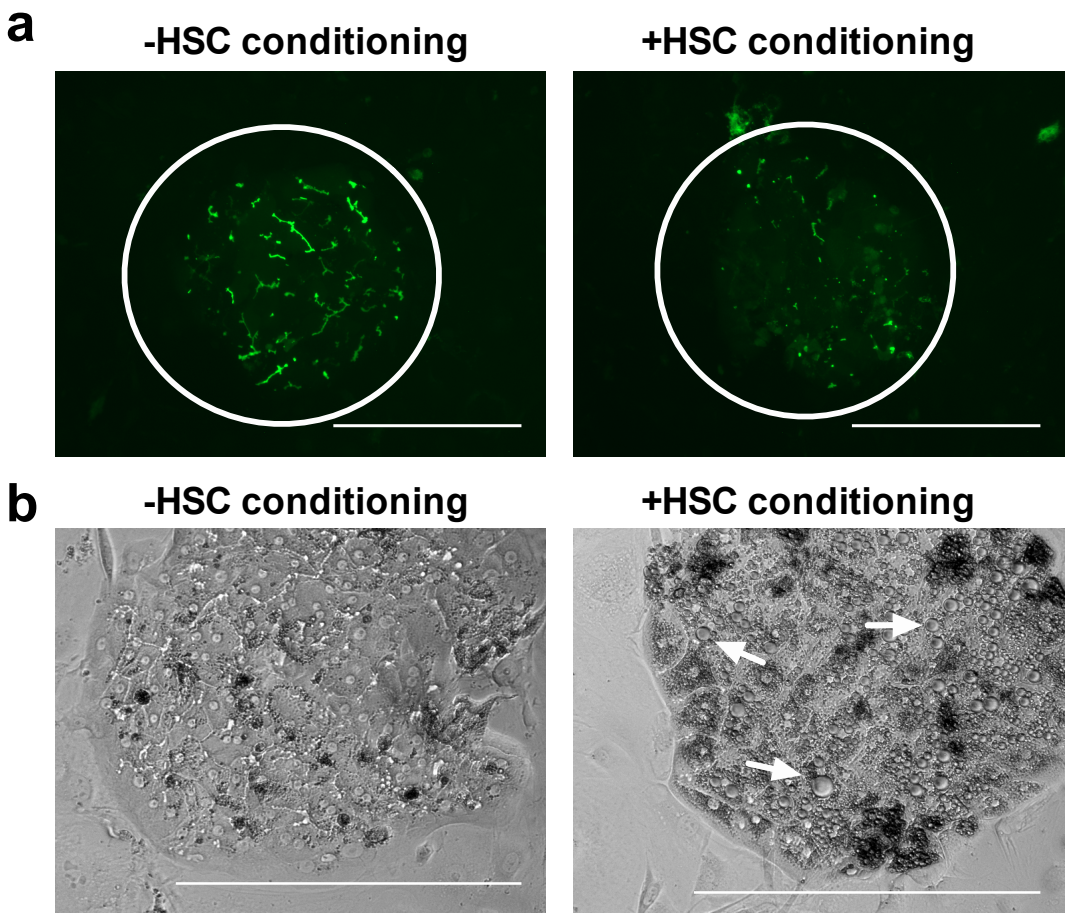

Supplemental Figure 7. Conditioned culture medium from activated HSCs causes loss of bile canaliculi and leads to steatosis in PHHs within MPCCs. Pure HSCs were cultured on collagen-coated tissue culture polystyrene concurrently to MPCCs in separate wells of a 24-well plate. Conditioned culture medium from the HSC cultures (initial seeding density of 5K cells per well) was filtered to remove cell contaminants and transferred to MPCCs every 2 days for ~2 weeks. **(a)** Representative images of PHH islands (denoted by white circles) in 2-week-old MPCCs (+/- treatment with HSC-conditioned medium) showing export of fluorescent dye (green) into the bile canaliculi between PHHs. **(b)** Representative phase contrast images of PHH islands in 2-week-old MPCCs (+/- treatment with HSC-conditioned medium). White arrows indicate macrovesicular steatosis in PHHs. Scale bars on images represent 400 μm.

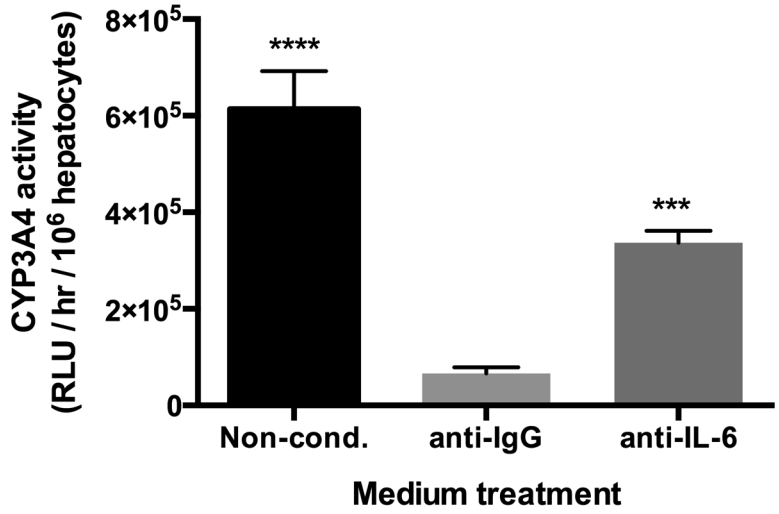

Supplemental Figure 8. Conditioned culture medium from activated HSCs causes downregulation of CYP3A4 in PHHs within MPTCs through IL-6 signaling (cultures were created using a different HSC donor than the one featured in the main figure 8). Conditioned culture medium from *pure* HSC cultures (initial seeding density of 5K cells per well) was filtered to remove cell contaminants and transferred to MPCCs every 2 days. HSC-conditioned culture medium was spiked with either an anti-IL-6 neutralizing antibody or its isotype-matched anti-IgG antibody control. MPCCs on day 3 of culture were then incubated with these conditioned media for 48 h and CYP3A4 activity was assessed on day 5 of culture. Statistical significance is displayed relative to the anti-IgG control. *** $p \leq 0.001$ and **** $p \leq 0.0001$.

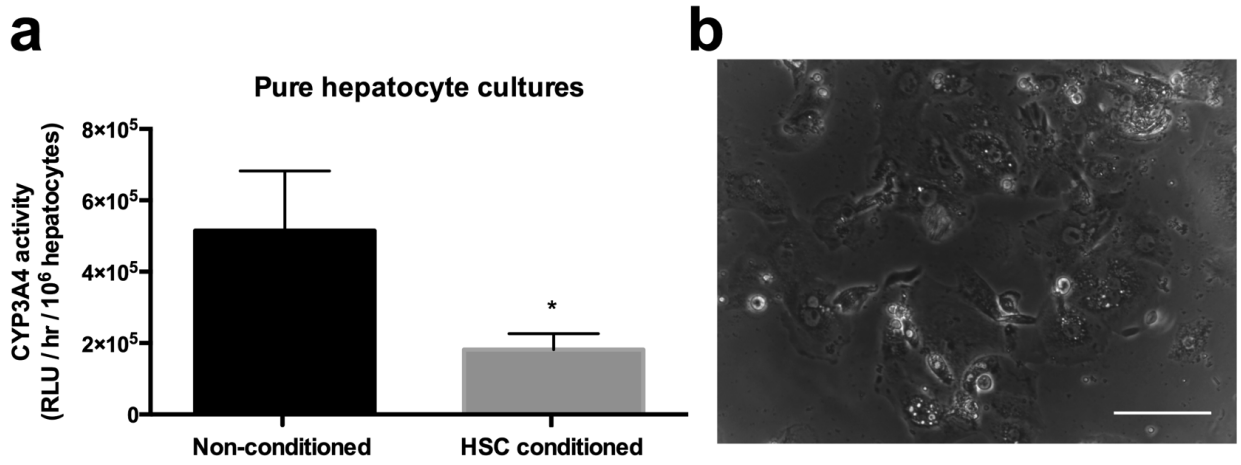

Supplemental Figure 9. Conditioned culture medium from activated HSCs leads to the downregulation of CYP3A4 activity in pure PHH monolayers. Pure HSCs (initial density of 5K cells per well) were cultured on collagen-coated tissue culture polystyrene concurrently to pure PHH monolayers (seeded on collagen-coated tissue culture polystyrene at 1.05M cells/cm^2) in separate wells of a 24-well plate. Conditioned culture medium from the HSC cultures was filtered to remove cell contaminants and transferred to PHH monolayers every 2 days for 6 days. **(a)** CYP3A4 activity in 6-day-old PHH monolayers (+/- treatment with HSC-conditioned medium). **(b)** Representative phase contrast image of a 6-day-old PHH monolayer. Statistical significance is displayed relative to 'non-conditioned' control. * p≤ 0.05. Scale bar on image represents 80 μm.

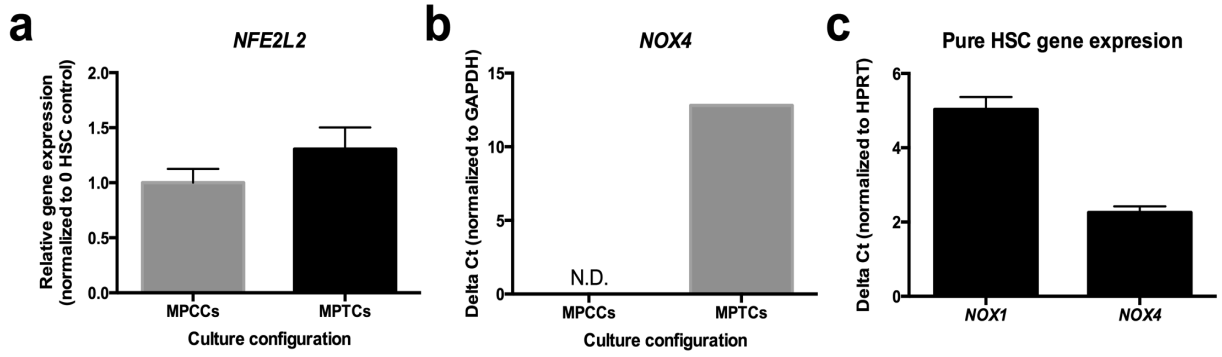

Supplemental Figure 10. Oxidative stress-related signaling in MPCCs, MPTCs, and pure cultures of activated HSCs. (a) *NFE2L2 (Nrf2) g*ene expression in 2-week-old MPTCs and MPCCs. **(b)** Delta Ct levels of *NOX4* gene expression in 2-week-old MPTCs and MPCCs (N.D. = not detected). *NOX1* was not detected in MPCCs or MPTCs (data not shown). **(c)** Delta Ct levels of *NOX1* and *NOX4* gene expression in 2-week-old pure HSC cultures. *GAPDH* was used as the housekeeping gene for panels 'a' and 'b', while *HPRT* was used as the housekeeping gene for panel 'c'.

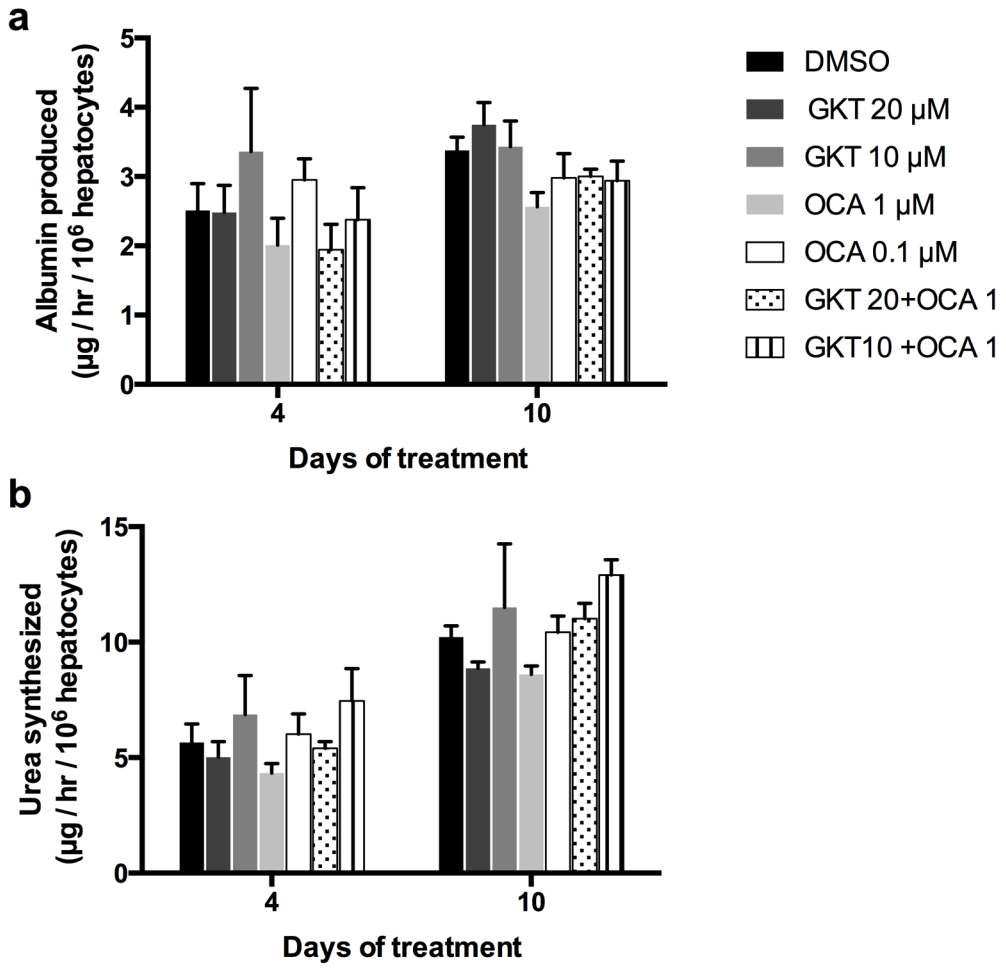

Supplemental Figure 11. Albumin and urea secretions in MPTCs treated with drugs and their combinations. (a) Albumin secretion over time in MPTCs (containing 2.5K HSCs) treated with vehicle control (DMSO), two doses of GKT, two doses of OCA, or a mixture of both GKT (20 µM and 10 µM) and OCA (1 µM) at the indicated doses. **(b)** Dosing as in panel 'a' except urea synthesis from MPTCs is shown.

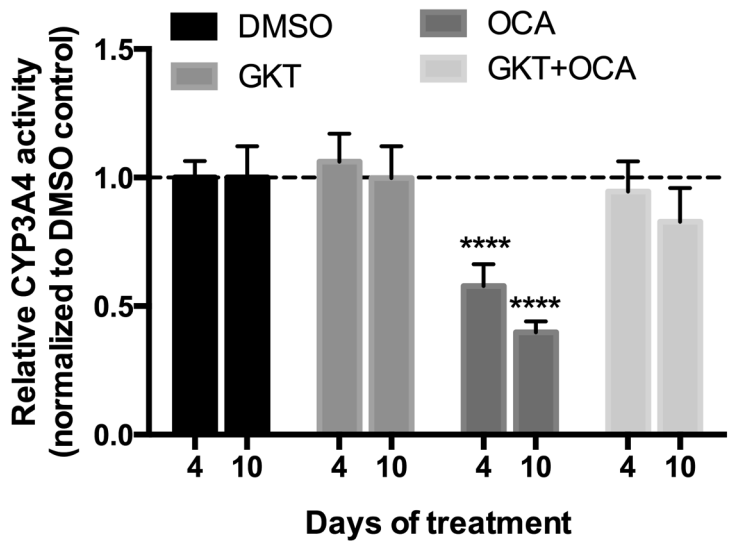

Supplemental Figure 12. CYP3A4 activity in MPCCs treated with individual drugs, drug combination, and the vehicle control. CYP3A4 activity over time in MPCCs treated with vehicle control (DMSO), 20 μM GKT, 1 μM OCA, and a mixture of both GKT (20 μM) and OCA (1 μM). Data is normalized to the CYP3A4 activity measured in DMSO-treated MPCCs. Statistical significance is displayed relative to the vehicle control for the respective time-point. **** $p \leq 0.0001$.

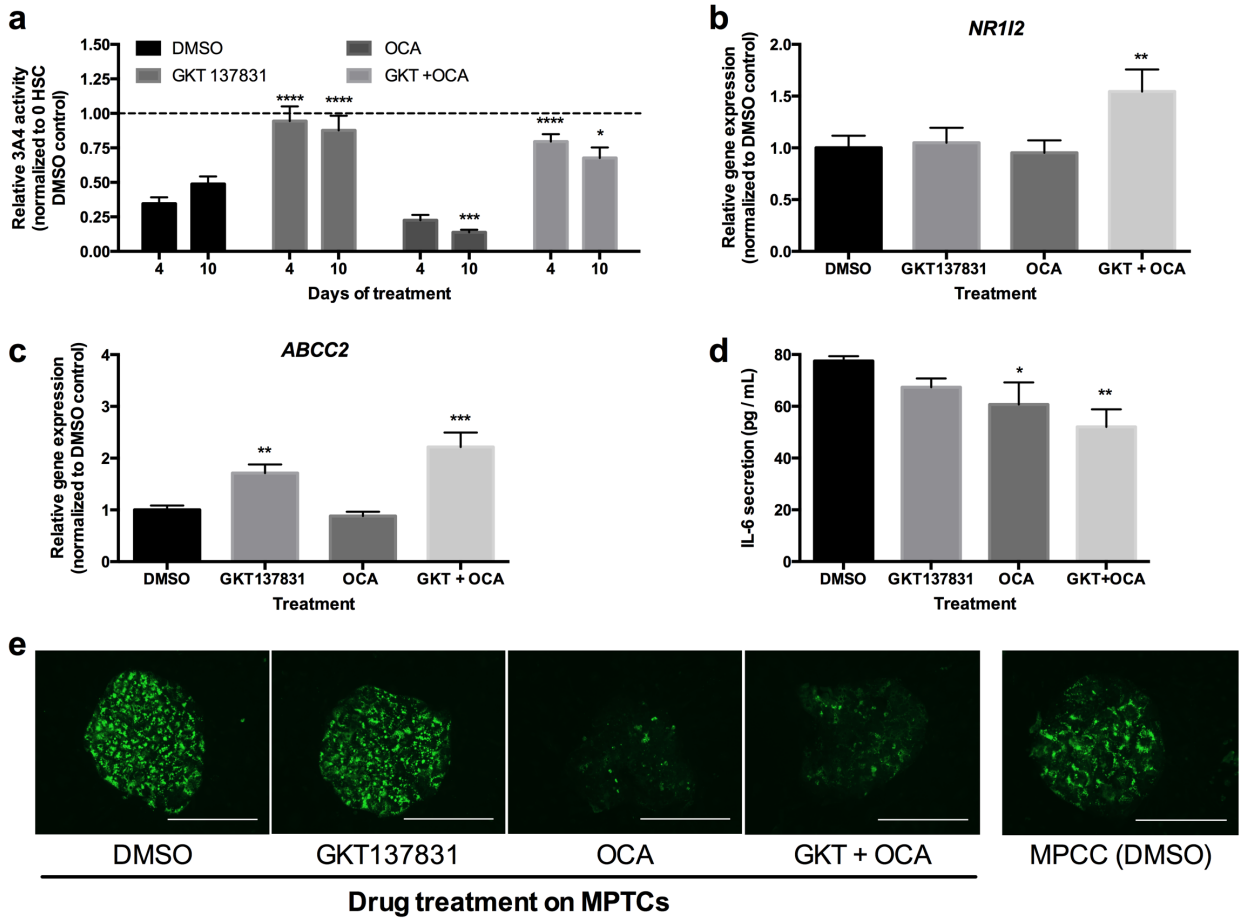

Supplemental Figure 13. Simultaneous inhibition of NOX4 and activation of FXR rescues PHH phenotype within MPTCs (cultures were created using a different HSC donor than the one featured in the main figure 9). (a) CYP3A4 activity in MPTCs treated for 4 d and 10 d with either DMSO, GKT137831, OCA, or a mixture of both drugs (GKT+OCA). Data is normalized to CYP3A4 activity in MPCC (0 HSC) controls (dashed line). **(b)** *NR1I2* (*PXR*) gene expression in drug-treated MPTCs relative to DMSO-treated MPTCs (10 d of treatment). **(c)** *ABCC2* (*MRP2*) gene expression in drug-treated MPTCs relative to DMSO-treated MPTCs (10 d of treatment). **(d)** IL-6 levels in drug-treated MPTC supernatants (6 d of treatment). **(e)** Neutral lipid (Nile red, green) staining of PHHs within MPTCs (10 d of drug treatment). DMSO-treated MPCC control image is shown to the far right. In all panels, statistical significance is displayed

relative to DMSO-treated MPTCs. * p≤ 0.05, ** p≤ 0.01, *** p≤0.001, and **** p≤0.0001. Scale bars on images represent 400 μm.